

STRUCTURE AND TOUGHENING MECHANICAL PROPERTIES OF MULTI PRINCIPAL COMPONENT HIGH ENTROPY ALLOY

by

Junhao DAI*

Department of Mechanical Engineering, Zhejiang Industry Polytechnic College,
Shaoxing, China

Original scientific paper
<https://doi.org/10.2298/TSCI2106019D>

At present, the strength and toughening degree of the multi-principal element high entropy alloy are not high, and the plastic deformation capacity is poor. In order to solve this problem, the structure and mechanical properties of the multi-element high entropy alloy were studied. The micro-structure and strengthening mechanism of the alloy were studied. By establishing a reliable random solid solution model and using the first principle to calculate the phase structure, thermodynamics, and elastic properties of the alloy, theoretical guidance is provided for the design and development of new high entropy alloy. The high entropy alloy system with high specific strength and high tensile plasticity was prepared, and its strengthening and toughening mechanism was studied. The experimental results show that with the increase of Zr content, the fracture strength of multi-component high entropy alloy first increases and then decreases. When it reaches a fixed value, the comprehensive mechanical properties of the alloy are the best. Compared with the two literature methods, the tensile strength of this method is 250 MPa, and the work hardening after yielding makes the alloy have higher strength and better plastic deformation ability.

Key words: multi principal component, high entropy alloy, structure, strengthening and toughening, mechanical properties, fracture strength, plastic deformation

Introduction

In the long process of human history, the development of materials has been accompanied by the progress of human civilization. As an important part of it, metal materials play an important role in the rapid development of modern civilization [1]. As a high entropy alloy (HEA) which breaks through the traditional alloy design concept, it has aroused great interest of researchers since its appearance, and has been widely used in practice [2].

As a new concept of alloy design, HEA is out of the scope of traditional alloy design. The HEA is an alloy formed by five or more equal or approximately equal metals [3]. The design idea of HEA covers the undeveloped space in the central area of multi-element alloy phase diagram. Based on its wide composition space, there are still many works to be improved in the design and research of HEA. At present, most of the multi-component HEA

* Author's e-mail: doojoo_hoo_zjipc@163.com

developed only have compression properties, but not room temperature tensile properties, which limits their wide application in practice.

The effect of cold rolling on the micro-structure and mechanical properties of coCrFeNiMn HEA containing Al and C was studied in [4]. Under the initial as cast condition, the alloy has face centered cubic single-phase coarse-grained structure. The micro-structure evolution is mainly related to the plane dislocation slip at relatively low deformation (up to 20%) or deformation twins and shear bands at high strain. In [5], the mechanical and thermodynamic properties of bisphenol F epoxy diglycidyl ether and flax fiber FRP composites modified by multi walled carbon nanotubes (MWCNT) were studied. The mechanical properties test showed that the tensile strength (48.7%) and tensile modulus (25.2%) of 1.0 wt.% MWCNT were significantly improved.

Based on the previous reasons, this paper chooses the multi principal component HEA as the research object, aiming to provide reference for the design and development of the follow-up high strength multi principal component HEA.

Structure and mechanical properties of multi principal component high entropy alloy

The effect of alloying on the phase composition of multi-component high entropy alloy system

The XRD pattern of multi principal component HEA system is shown in fig. 1. From fig. 1(a), it can be seen that M0V10-M10V10 all form a single BCC structure. When Mo content increases to M13V10, a weak diffraction peak appears on the left side of (110) diffraction peak [6, 7]. In order to see more clearly the change of, (110) peak with Mo addition, enlarge this area to get fig. 1(b). With the addition of Mo (110), the diffraction peak shifts to the right, which is described by Bragg equation:

$$2d \sin \theta = n\lambda \quad (1)$$

where d is the crystal surface spacing, θ – the diffraction angle, and λ – the ray wavelength.

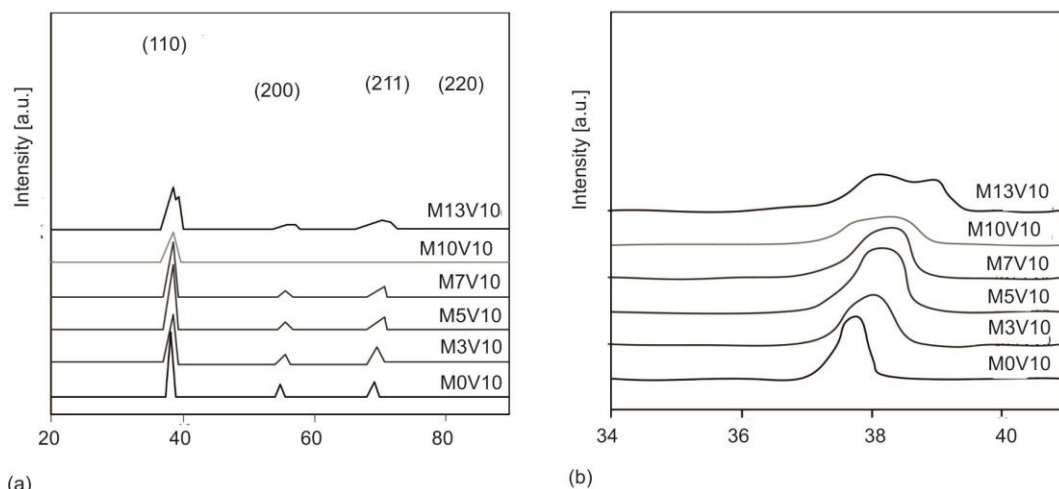


Figure 1. The XRD analysis of multi principal component HEA; (a) XRD atlas and (b) the X-ed pattern of the (110) diffraction peak of Miller index

The diffraction angle reflects the size of the crystal face spacing. The larger the diffraction angle is, the smaller the crystal face spacing is. The crystal face spacing of BCC structure is proportional to the lattice constant. The addition of Mo reduces the lattice constant of the alloy [8]. This is related to the atomic radius of Mo. It can be seen from tab. 1 that the atomic radius of V is the smallest, followed by Mo. Therefore, Mo reduces the lattice constant of the alloy. At the same time, the addition of Mo reduces the diffraction intensity and broadens the diffraction peak. The addition of components leads to serious lattice distortion, thus strengthening the scattering effect, leading to the decrease of diffraction intensity, and the serious lattice distortion leads to the decrease of crystal structure symmetry, which further widens the diffraction peak [9, 10].

Table 1. Energy spectrum at different positions of multi principal component HEA

Alloys	Rehion	Chemical compositions/position [%]				
		Ti	Zr	Nb	V	Mo
M0V10	Nominal	25	25	25	25	–
	O	26.30	25.92	21.40	26.38	–
M3V10	Nominal	23.26	23.26	23.26	23.26	6.97
	DR	23.75	16.69	27.86	22.61	9.09
	IR	23.79	23.62	21.97	24.30	6.32
M5V10	Nominal	18.87	18.87	18.87	18.87	24.52
	DR	17.99	15.97	22.46	19.16	24.42
	IR	18.52	20.17	20.17	19.06	22.08
M7V10	Nominal	17.54	17.54	17.54	17.54	29.82
	DR	16.07	6.19	19.16	15.43	43.15
	IR	18.23	24.99	13.36	16.02	27.41
	PT	16.89	42.82	5.85	15.65	16.06

Compression properties at room temperature

In G-MV3 alloy system, with the increase of Mo content, the change trend of compression property at room temperature is different from that of G-MV10. As there is no precipitation of the second phase, the yield strength continues to increase, the amount of plastic deformation decreases, and there is no turning point. Among them, M3V3 alloy has the best comprehensive properties. It can be seen from the XRD phase analysis and SEM structure observation that there is only a single BCC phase in G-MV3 alloy system. Because of the addition of Mo element with high bulk modulus, the yield strength of the alloy increases. In the multi-component alloy system, the V element can strengthen the alloy, but in order to ensure good plastic deformation ability, the V content needs to be reduced.

Experimental analysis

Preparation of experimental materials

Three kinds of Fe-Mn-Al-Si alloys are designed in the experiment. They are melted into alloy ingots in vacuum induction furnace. According to the mass percentage content of main alloy elements Mn, they are named as 20 Mn alloy, 25 Mn alloy and 29 Mn alloy, respectively. The results of chemical composition analysis are shown in tab. 2. Among them, 20 Mn alloy produces TRIP effect when it is deformed at room temperature, which is called TRIP alloy; 29 Mn alloy produces TWIP effect when it is deformed at room temperature, which is called TWIP alloy and 25 Mn alloy is between them. The Mn was measured by titration (NACIS/CH065:2005), Al by ICP-AES (NACIS/CH008:2005), Si by weight

(GB/T223.60-1997), and C by infrared absorption (GB/T20123-2006). The total content of P and S harmful elements in the two alloys is less than 0.01%.

Table 2. Chemical composition of three Fe-Mn-Al-Si Alloys (Mass percentage, wt.%)

	20 Mn alloy	25 Mn alloy	29 Mn alloy
Mn	20.3	25.02	28.98
Al	2.64	2.52	2.53
Si	2.64	2.75	2.70
C	0.006	0.0062	0.011
Fe	Bal.	Bal.	Bal.

Structural structure and mechanical properties of multi principal component high entropy alloy

Quasi static uniaxial tensile test

Due to the existence of oxide scale and inclusions on the surface of cold rolled and annealed specimens, in order to eliminate the influence of oxide scale and inclusions on the experimental results, the oxide scale and inclusions on the surface of specimens should be removed with sandpaper before tensile test.

In this paper, MTS Landmark 50/100 kN electro-hydraulic servo fatigue testing machine is used for room temperature tensile test, and the tensile rate is 3 mm per minute. According to GB/T 228-2002 standard, the tensile specimen is prepared by wire cutting.

Impact test

The V-notch impact specimen is prepared by wire cutting, and its size is 55 mm × 10 mm × 2.5 mm. Before the impact test, all the impact samples were fully recrystallized and annealed at different temperatures to ensure the homogeneity of the sample structure before the impact test. The impact test was carried out on JB-300B pendulum impact test machine, and the test temperatures were 200 °C, 80 °C, 20 °C, 80 °C, and 190 °C, respectively. Immerse the low temperature impact sample in the mixture of alcohol and liquid nitrogen at a certain temperature in advance, and take out the sample for rapid impact after holding for 10 minutes. The high temperature impact sample is kept in the heating furnace for 10 minutes, and then taken out for rapid impact. The impact process is shown in fig. 2.

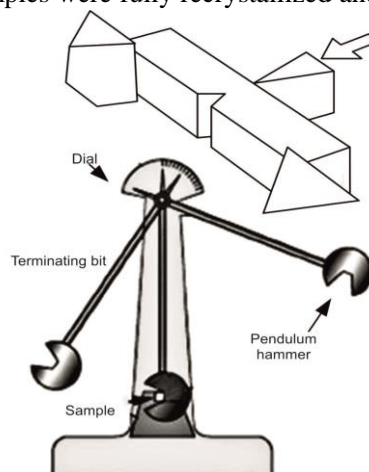


Figure 2. Schematic diagram of impact test

Microhardness test

The micro Vickers hardness tester (HXD-1000T) was used to test the hardness. The indenter of the hardness tester is in the shape of positive pyramid and the face angle is 136°. The measuring principle of the hardness tester is: first, measure the length of two diagonals, respectively, and calculate the average value d , from which we can know the surface area of the indentation, and then use the load divided by the surface area to obtain the microhardness. The calculation:

$$HV = 0.102 \frac{2F \sin \frac{136^\circ}{2}}{d^2} = 0.1891 \frac{F}{d^2} \quad (20)$$

The samples were roughed and finely ground with 1000 #, 2000 #, and 5000 # sandpaper to remove the oxide layer on the surface, and then polished with 2.5 μm diamond abrasive paste to remove the fine scratches on the surface of the samples. Finally, the surface stress layer was removed by electropolishing. The hardness test sample is a small square of 10 mm × 10 mm × 1 mm, and the hardness test area is the center of the sample. Each sample is tested at eight points, the maximum and minimum values are removed, and then the average value is taken. The general test conditions are: loading load is 4.9 N, loading time is 15 seconds. The sample of Streptococcus MG titer is a cross-section sample. Its hardness is measured from the surface of the sample to the center of the sample in a straight line. The loading load is 0.49 N and the loading time is 15 seconds. The length of the two diagonals is measured manually and the hardness value is calculated.

Analysis of experimental results

The following experimental results are obtained by using the mechanical properties test of the above multi principal component HEA, as shown in fig. 3.

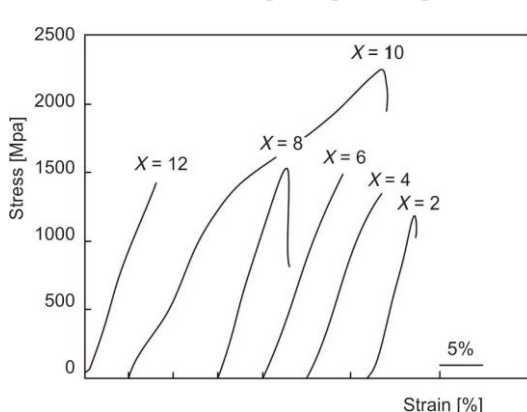


Figure 3. Quasi-static compression stress-strain curve of multi principal component HEA

Figure 3 shows the compression stress-strain curve of the multi-component HEA at room temperature and tab. 3 shows the corresponding mechanical property parameters. It can be seen from the chart that with the increase of Zr content, the fracture strength of the alloy increases first and then decreases. When X = 10, the comprehensive mechanical properties of the alloy are the best, the yield strength is 1180 MPa, the fracture strength is as high as 2300 Mpa, and the plastic deformation is 11.6%. The work hardening after yield makes the alloy have high strength and good plastic deformation ability at the same time. The strength and plasticity of alloy samples with X = 12, 8, 6,

4, and 2 are not as good as those of the former, and there is no obvious work hardening behavior, showing obvious brittle fracture. It can be seen that the mechanical properties of the alloy system cannot be improved by substituting Ni element for Zr element in the system except for the alloy with X = 10.

Table 3. Compression mechanical property parameters of multi principal component HEA

X value	Yield strength [Mpa]	Fracture strength [Mpa]	Plastic strain [%]
12	–	1435	1.45
10	1185	2300	11.6
8	1000	1570	1.38
6	1180	1535	1.34
4	950	1400	1.46
2	–	1255	1.48

Discussion

The main three creative achievements of this paper are:

- Based on the establishment of reliable random solid solution model and the first principle calculation simulation, the multi-component high stripping alloy of TiZrNbHf with tensile plasticity and excellent thermal stability was predicted and developed. The tensile strength and plasticity of TiZrNbHf multi-component HEA were improved simultaneously by the addition of oxygen.
- A series of TiZrNbMoW multi-component HEA with high specific strength and compression plasticity were developed by adjusting the Mo content of high modulus element. Among them, TiZrNbMo0.3W0.3 multi-component HEA has specific strength up to 198 MPa·m³/kg and compression plasticity over 50%.
- The potential application of TiZrNbHf multi-component HEA at high temperature was improved by adding Al. The addition of 5% Al can significantly improve the strength of the alloy, maintain the tensile plasticity and excellent thermal stability, and provide an excellent prototype alloy for the future application of multi principal component HEA at high temperature.

In order to verify the effectiveness of the micro-structure and properties of the multi principal component HEA, the method proposed in [4, 5] was used as the contrast object. The experimental results are shown in fig. 4.

It can be seen from fig. 4 that the maximum tensile strength of the two literature methods is 250 Mpa. Compared with the two literature methods, the tensile strength is higher and the mechanical properties of the HEA are better.

Conclusion

In this paper, a study on the structure and mechanical properties of multi principal component HEA is presented.

The first principle method is used to calculate the thermodynamic and elastic properties of TaNbMoW and TiZrNbHf multi-component HEA. The plasticity potential of TiZrNbHf multi-component HEA is predicted. The high specific strength and room temperature compression plasticity of the TiZrNbMoW multi-component HEA obtained in this paper are verified by experiments. The effects of Mo and V alloying on the micro-structure and phase stability of the alloy system are studied. The addition of O can greatly improve the strength of TiZrNbHf multi-component HEA and keep the tensile plasticity of the alloy. The effect of Al addition on the micro-structure, phase stability and mechanical properties of TiZrNbHf multi-component HEA was studied. The results show that with the increase of Zr content, the fracture strength of the multi principal component HEA increases first and then decreases. When it reaches a certain fixed value, the comprehensive mechanical properties of the alloy are the best. The work hardening after yield makes the alloy have high strength and good plastic deformation ability. The alloy can fully meet people's demand for metal material properties, and

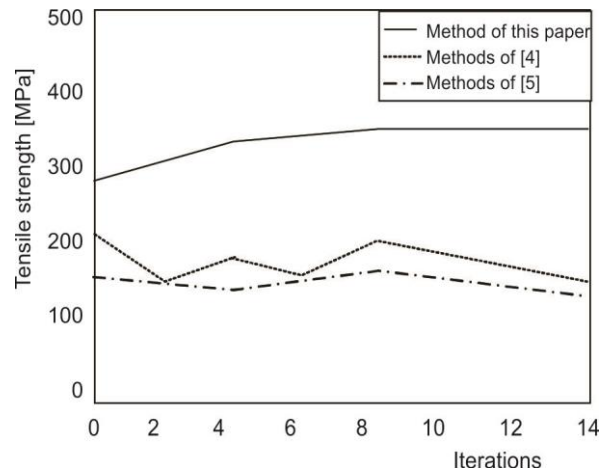


Figure 4. Compare the experimental results

needs to be further applied in related industries to promote the further development of machining industry. In this study, only the structure and toughening mechanical properties of HEA were studied. In the future, the effect of HEA in practical application was studied.

Acknowledgment

This research has been financed by the Scientific Research Project in 2019 of the Department of Education of Zhejiang Province - Research on the Laser Strengthening Technology of Zinc Alloy Reduction Rolls (No. Y201941534).

References

- [1] Zhang, H., *et al.*, Effect of High Configuration Entropy and Rare Earth Addition on Boride Precipitation and Mechanical Properties of Multi-Principal-Element Alloys, *Journal of Materials Engineering and Performance*, 26 (2017), 8, pp. 1-6
- [2] Cao, J., *et al.*, The Impact of the Cross-Shareholding Network on Extreme Price Movements: Evidence from China, *Journal of Risk*, 22 (2019), 2, pp. 79-102
- [3] Jo, M. G., *et al.*, Microstructure and Mechanical Properties of Friction Stir Welded and Laser Welded High Entropy Alloy Crmnfeconi, *Metals & Materials International*, 24 (2018), 1, pp. 73-83
- [4] Klimova, M., *et al.*, Microstructure and Mechanical Properties Evolution of the Al, C-Containing Cocrfenimn-Type High-Entropy Alloy during Cold Rolling, *Materials*, 11 (2017), 1, pp. 53-66
- [5] Wang, H. G., *et al.*, Mechanical and Thermodynamic Properties of Unidirectional Flax Fiber Reinforced Cnt Modified Epoxy Composites, *Fibers and Polymers*, 20 (2019), 6, pp. 1266-1276
- [6] Chen, Y., *et al.*, Aging Mechanism and Equivalent Acceleration Relationship of g827/3234 Composite in the Marine Environment, *Fuhe Cailiao Xuebao/Acta Materiae Compositae Sinica*, 35 (2018), 12, pp. 3304-3312
- [7] Ponton, P. I., *et al.*, Effects of Low Contents of a2m3o12 Submicronic Thermomiotic-Like Fillers on Thermal Expansion and Mechanical Properties of Hdpe-based Composites. *Polymer Composites*, 39 (2018), S3, pp. E1821-E1833
- [8] Zhang, M., *et al.*, Microstructure and Mechanical Properties of a Refractory Cocrmonbti High-Entropy Alloy, *Journal of Materials Engineering & Performance*, 26 (2017), 8, pp. 1-9
- [9] Tseng, K., *et al.*, A Light-Weight High-Entropy Alloy al20be20fe10si15ti35, *Science China Technological Sciences*, 61 (2018), 2, pp. 184-188
- [10] Shang, X. L., *et al.*, Effect of Mo Addition on Corrosion Behavior of High-Entropy Alloys Cocrfenimox in Aqueous Environments, *Acta Metallurgica Sinica (English Letters)*, 32 (2019), 1, pp. 41-51